Archives of Civil and Mechanical Engineering (2025) 25:69
https://doi.org/10.1007/s43452-025-01132-7

ORIGINAL ARTICLE

Seawater-mixed concretes containing supplementary cementitious materials: compressive strength, e-modulus, electrical resistivity, and life cycle assessment

Sundar Rathnarajan[1] · Joao Nuno Pacheco[2,3] · Francisco Capucha[2] · Javier Valencia[2,3] · Mateusz Techman[1] · Pawel Sikora[1]

Received: 4 August 2024 / Revised: 4 December 2024 / Accepted: 8 January 2025
© The Author(s) 2025

Abstract
Water and concrete are the materials humans consume the most on earth. By 2040, several countries are expected to face extreme water stress and the need for significant growth in their infrastructure simultaneously. Water is a fundamental ingredient for concrete production, and the need for infrastructure growth can further increase the water demand for concrete production and thus affect these regions facing water scarcity. Including supplementary cementitious materials (SCMs), non-metallic fibres, and coated/polymer reinforcements can increase the feasibility of producing concrete with seawater (SW). There is a lack of information on the long-term strength and durability properties of SW-mixed concretes (SWC) produced with SCMs. This paper optimises binder compositions with CEM I, fly ash, ground granulated blast furnace slag (slag), and metakaolin suitable for adapting SWC based on performance indicators. Binary and ternary blended concretes of similar binder content (360 kg/m^3) and w/b (0.45) were designed and cast with the SCMs mentioned above. Compressive strength, surface resistivity, and accelerated carbonation tests were conducted on the concrete produced with freshwater (FW) and seawater (SW). SWC produced with 30% slag and 15% metakaolin had higher electrical resistivity and an improvement in compressive strength (up to 30%) than other combinations used for producing SWC. Life cycle assessment identified that the concretes produced with fly ash, and ternary combination of fly ash and metakaolin had the least water depletion potential (WDP) compared to other SW-mixed concretes. Also, the replacement of FW by SW reduces the WDP up to 50%.

Keywords Seawater-mixed concrete · Supplementary cementitious materials · Long-term compressive strength · Resistivity · Accelerated carbonation

1 Introduction

The United Nations (UN) World Water Development Report 2024 states that roughly half of the human population faces severe water scarcity at least a few parts of every year [1]. World Resources Institute identified the 25 countries including India, middle eastern nations, and a few countries from Africa that face extremely severe water stress, indicating that their annual water withdrawal exceeds at least 80% of their renewable freshwater resources [2]. The freshwater availability is shrinking in contrast to the yearly increase in water demand. Also, the deterioration in water quality of available water resources can further increase the global water demand unequally across regions [3]. Global industrial water demand is expected to rise between 70 and 120% by 2050 compared to 2010 [4]. Approximately one-tenth of industrial water consumption is attributed to concrete production, the world's most consumed construction material. Among that, 75% of the water demand for concrete occurs in the regions facing severe to extreme water stress [5]. Water consumption in concrete includes not only the amount of water required for the processing of raw materials (e.g. cement manufacturing and aggregate washing), but

✉ Sundar Rathnarajan
sundarrathinaraj@gmail.com

✉ Pawel Sikora
pawel.sikora@zut.edu.pl

1 Faculty of Civil and Environmental Engineering, West Pomeranian University of Technology, Szczecin, Poland

2 c5 Lab – Sustainable Construction Materials Association, Linda-a-Velha, Portugal

3 CERIS, Av. Rovisco Pais, 1049-001 Lisbon, Portugal

Published online: 27 January 2025

also the water used as a raw material in the concrete mix. Even though standards allow the use of recovered water for concrete production (such as the washing water of trucks and equipment of ready-mixed concrete plants – e.g. EN 1008), potable/freshwater (FW) is still preferred for reinforced concrete applications [6]. Using alternative reinforcements and supplementary cementitious materials (SCMs) could allow us to use alternative water sources for concrete production since corrosion-related durability concerns will no longer be a problem, which may be a limiting factor for producing concrete with non-potable water [7].

Using seawater in concrete production is not entirely new, considering that Roman concretes were often made of lime, volcanic ash (pozzolanic), and seawater (SW) [8]. Researchers have recently attempted to mimic the binding mechanism of ancient Roman seawater concrete using calcined clays, indicating the acceleration in binder reactivity and more strength development with higher alumina content [9]. The possibility of producing irreversible bound chloride phases like Friedel's salt can be higher with SCMs like metakaolin with more Al_2O_3 (> 40%), and thus, the availability of free chlorides to initiate onset of corrosion in embedded reinforcement could be curtailed [10]. Optimising the binder composition for achieving an improved strength and maximum chloride binding with SCMs in concretes produced with seawater mixing is needed.

The replacement of FW with SW improved the mechanical properties of seawater-mixed concrete (SWC) produced with CEM I were increased at early ages (7 and 28 days) [11] and impaired slightly at a later age (beyond 90 days) [12]. The accelerating effect of seawater on the hydration kinetics of cementitious systems had an unintended impact on the workability of SWC [13] with the initial slump flow reducing by 20% compared to FW-mixed concrete [14]. The plastic viscosity and yield stress of the SW-mixed cement pastes were higher than the FW-mixed counterparts, which could be attributed to the faster hydration in the presence of suspended chloride ions [15]. Furthermore, the increase in viscosity and yield stress is larger in cement pastes with SCMs having higher alumina content [15]. The drying shrinkage strain in SWC can be increased by 10–15% due to the presence of hygroscopic salts in mixing water and denser microstructure with smaller pore sizes, leading to higher capillary stress compared to the FW-mixed concrete (FWC) [16].

Concerning the influence of SW on durability, the water-accessible porosity and water absorption coefficient of SW-mixed mortars with nano-SiO_2 were reduced due to the synergistic effect of accelerated hydration and enhanced pozzolanic reaction in cementitious matrix [17]. The water penetration depth of SW-mixed concrete was less than that of ordinary concrete due to the reaction between Friedel's salt and portlandite in the cementitious matrix to form $CaCl_2$ and improve the compactness of the concrete [18]. The freeze–thaw resistance of SWC was found to be higher compared to FWC [19]. More Na^+ and K^+ ions in pore solution of SW-mixed mortars could increase the risk of alkali–silica reaction (ASR) [20]. The chloride binding mechanism in cementitious matrices containing SCMs is complex to model due to the wide range of blended combinations being developed towards low-carbon cements for improved sustainability [21]. Unlike the later age Cl^- binding in FW-mixed cementitious systems exposed to chloride-laden environment, the Cl^-binding in SW-mixed cementitious systems can occur during the early hydration (within 48 h) by interacting with C_3S and C_3A phases [22]. The improved ability to bind chlorides at early ages itself in cementitious matrix of seawater-mixed and sea-sand UHPC with metakaolin is expected to mitigate the corrosion of steel [23]. However, the chemical binding of chlorides can be undone partially or completely, and the physical binding of chlorides can be lost partially with the carbonation of hydrated cement phases [24], and henceforth, understanding the carbonation resistance of SW-mixed concrete is essential.

Seawater as mixing water for concrete was found to have less corrosion activity than seawater for both mixing and curing concrete in Dasar et al. [25] due to the saturation in chloride binding ability and presence of higher free chlorides. Furthermore, concretes with inclusion of slag and fly ash demonstrate a lower macrocell corrosion than CEM I concrete mixed with seawater [26]. Beyond the incorporation of SCMs, the onset of corrosion in SWC can be controlled by adding corrosion inhibitors that influence the anodic and cathodic reactions at the near-surface interface [27]. Thus, incorporating SCMs can improve the long-term durability of SWC compared to the concrete made with SW and CEM I. Furthermore, the use of SW in concrete mixing can lessen the water footprint in concrete production by 10–50% and can reduce the global warming potential [28]. Rathnarajan et al. [29] focused on optimising the binder compositions for concrete made with SW by studying binary and ternary blended concrete compositions, with emphasis based on strength improvement and setting time. However, limited research works are available to determine the long-term strength, durability, and sustainability potential of SW-mixed concretes with SCMs. To summarise, the motivation for this study is to develop and evaluate the strength, durability, and sustainability characteristics of SWC with SCMs to combat the freshwater crisis in countries facing severe water stress.

2 Research significance

The research focus on SW-mixed concretes in recent years coincides with the UN-Water action decade (2018–2028), emphasising the sustainable and integrated management of freshwater resources. Despite some early investigations,

there is a lack of systematic studies concentrating on the evolution of long-term strength and durability of SWC produced with SCMs. The current work compares the strength and resistivity measurements on 1, 7, 28, and 91 days in selected binary and ternary combinations (10 mixes) to identify the most suitable ternary blended cementitious combination suitable for producing SWC. The surface and bulk resistivity measurements up to 91 days in SWCs can indicate the resistance against the further ingress of aggressive ions indirectly (a prerequisite for establishing a database to develop correlations between resistivity and other long-term durability properties of SWC). Also, this study evaluates the carbonation resistance of the SWCs to understand the risk of reversal of chloride binding with the formation of carbonated products. Furthermore, the global warming potential (GWP) and water depravity potential (WDP) of the proposed SWCs could help understand their contributions to improving the sustainability of concrete production. It is a first-of-its-kind work assessing and identifying the most suitable binary/ternary blended SW-mixed concretes based on engineering and sustainability parameters. Finally, this work outlines the need for conducting further experiments on SWC exposed in sulphate and chloride-rich environments to derive the correlation between the durability indicators like resistivity and long-term diffusion and migration of aggressive ions.

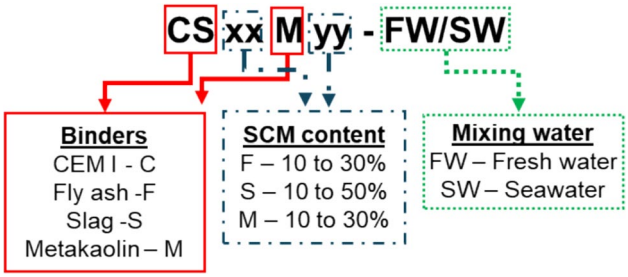

Fig. 1 Nomenclature of the concretes

Table 1 Chemical and physical properties of CEM I and SCMs in this study

Oxides	CEM I (C)	Fly ash (F)	Slag (S)	Metakaolin (M)
CaO	64.5	2.6	35.6	2.5
SiO_2	21.2	46.3	33.8	55.4
Al_2O_3	6.1	26.1	17.4	32.1
Fe_2O_3	2.4	5.1	1.0	2.4
MgO	1.3	1.0	8.0	1.5
MnO	1.8	0.6	0.5	0.6
K_2O	0.4	4.9	0.6	1.4
SO_3	2.1	0.6	-	2.3
Na_2O	0.2	0	0.4	-
LOI	2.4	2.4	3.1	3.1
S.G[1] (g/cm^3)	3.12	2.05	2.88	2.50
d_{50} (μm)	17.9	36.7	18.6	8.1

3 Materials and methodology

3.1 Raw materials

A total of 10 binder compositions were tested. CEM I 42.5 R conforming to EN 197-1 [30] was used as the primary binder throughout this study. Siliceous fly ash (F), ground granulated blast furnace slag (S), and metakaolin (M) were used as SCMs in various proportions in binary and ternary compositions of binder, as indicated in Fig. 1. Table 1 lists the chemical oxide composition and physical properties of this study's CEM I and SCMs. River sand with a maximum particle size of 2 mm was utilised as the fine aggregate. The coarse aggregate was rounded gravel of two particle size distributions (2/8 mm and 8/16 mm). The total binder content and water-to-binder (w/b) ratio of the concrete mixes were kept constant at 360 kg/m^3 and 0.45. Tap water was used as a source of freshwater (FW). Artificial seawater (SW) was prepared according to ASTM D1141 [31]. A polycarboxylate (PCE)-based superplasticiser (SP) was used to produce concretes with workability, not only complying with the S2 slump class but also ensuring that all mixes had similar flow (the slump of all mixes was between 65 and 75 mm—see Table 2). An increased SP dosage of 10% was required to achieve concrete with similar slump values.

Figure 1 shows the nomenclature of the concrete mixes evaluated in this study. The first part of the nomenclature represents the type of binder, followed by the percentage of cement replacement by each type of SCM used. The last part of the name represents the type of mixing water.

3.2 Experimental methodology

Table 2 presents the mix proportion details of the 20 concretes in this study. Table 2 also lists the slump values of the concretes measured according to EN 12350-2 [32]. The slump values of concretes produced with SW were lower than FW counterparts at same SP dosage. The SP dosage was increased up to 10% in SWC to produce concrete of similar consistency for casting. These concretes were subjected to compressive strength, elastic modulus, surface resistivity, bulk resistivity, accelerated carbonation tests, and life cycle assessment.

Table 2 Concrete mix proportion details and consistency of mixes

Mix ID	Quantity of raw materials (kg/m^3)										Slump (mm)	
	CEM I	FW/SW	F	S	M	River sand	CA 8/16 mm	CA 2/8 mm	SP dosage			
									FW	SW	FW	SW
CC-FW/SW	360	162	–			732	703	469	5.0	5.6	75	70
CF30-FW/SW	252	162	108	–		717	690	460	5.0	5.4	75	72
CS50-FW/SW	180	162	180	–		726	698	466	5.4	6.1	70	65
CM30-FW/SW	252	162	108	–		722	695	463	7.6	8.2	65	60
CS20F10-FW/SW	252	162	36	72	–	724	697	465	5.1	5.4	75	75
CS30F15-FW/SW	198	162	54	108	–	721	694	462	5.8	6.1	70	68
CF20M10-FW/SW	252	162	72	–	36	718	691	461	6.5	6.8	70	65
CF30M15-FW/SW	198	162	108	–	54	712	685	457	7.0	7.2	75	65
CS20M10-FW/SW	252	162	–	72	36	726	698	466	6.5	6.8	75	70
CS30M15-FW/SW	198	162	–	108	54	723	696	464	7.0	7.2	75	68

Note: SP superplasticiser, *F* fly ash, *S* slag, *M* metakaolin, *CA* coarse aggregate

3.2.1 Compressive strength

Concrete cubes of size 100 mm were prepared and cured under water immersion for 1, 7, and 28 days. The testing equipment had a maximum capacity of 5000 kN, and the load rate complied with EN 12390-3 [33]. Three replicates of concrete cubes were tested at each age of curing mentioned above and on 91st day. The mean and the standard deviation values are reported.

3.2.2 Elastic modulus

Concrete cylinders of diameter 100 mm and height 200 mm were cast and cured for 1 and 28 days. On 1st and 91st days, the compressive strength of the cylinder was evaluated, and three levels of load corresponding to 0.5 MPa, 15% of the compressive strength, and one-third of the compressive strength were imposed in three cycles, as mentioned in EN 12390–13 [34]. The strain in the specimens was measured using three extensometers located at an angle of 120° to each other. The strain values plotted against three specimens' stress and modulus of elasticity were calculated in each concrete mix.

3.2.3 Surface resistivity

Concrete cylinders of diameter 100 mm and height 200 mm were used to determine the surface resistivity (ρ_S) using the Wenner 4-probe resistivity method conforming to AASHTO T 358 [35]. The surface resistivity measurements were taken from the specimens immersed in water for 1, 7, 28, and 91 days. The Wenner 4-probe method works with the principle that current (I) was applied to the saturated surface of concrete using two outermost probes, and the potential difference (V) was measured using two inner probes. The current can be transmitted through the porous network of concrete with the help of ions in the pore solution. The spacing of the probes (a) used in this study is 38 mm, and the surface resistivity of the concrete was calculated as mentioned in Eq. 1. Surface resistivity values were measured at three different locations in the circumference of each of the three concrete cylinders, and from these 9 data points, the mean and deviation are reported.

$$\text{Surface resistivity, } \rho_s = 2\pi a \frac{V}{I} [\text{k}\Omega.\text{cm}]. \quad (1)$$

3.2.4 Bulk resistivity

The bulk resistivity was determined by passing an alternate current (AC) signal through the hardened concrete with the help of two parallel electrode plates coupled with a Wenner-4-probe resistivity meter. Two discs were placed on the top and bottom surfaces of the concrete cylinder (100 mm diameter and 200 mm height) with a moist sponge to provide a saturated surface. The total resistance measured by the instrument is the sum of resistance from concrete and two sponges. The bulk resistance of concrete (R_{CY}) is calculated by subtracting the resistance of sponges from the total resistance, and this value is further processed as provided in Eq. 2 to calculate the bulk resistivity of the concrete. The spacing between the probes or electrodes (a) is also an independent variable in Eq. 2. Equation 3 defines the factor 'K', which is calculated using the area and length of the concrete cylinder.

$$\text{Bulk resistivity, } \rho_b = R_{CY} \frac{K}{2\pi a} [\text{k}\Omega.\text{cm}], \quad (2)$$

$$K = \frac{\text{Area of cylinder}}{\text{Length of cylinder}}. \quad (3)$$

3.2.5 Accelerated carbonation tests

The accelerated carbonation was carried out according to the Portuguese specification LNEC E391 [36]. The tests were carried out on concrete specimens with a diameter of 100 mm and a depth of 40 mm. The specimens were cured in immersion until 14 days before exposure to carbonation. During these 14 days, the specimens were stored in a dry chamber. The accelerated carbonation conditions were: CO_2 concentration: 5% by volume; temperature: 23 ± 3 ºC; and humidity: 60 ± 5%. Three specimens were tested after 28 days of accelerated carbonation. After exposure, the specimens were cut and sprayed with phenolphthalein solution to determine the carbonation depth. The average carbonation depth from three concrete discs was measured and reported with standard deviation.

4 Results and discussions

4.1 Compressive strength development

Figure 2 shows compressive strength evolution in FW/SW-mixed concretes up to 91 days. The solid lines represent the strength evolution in FW-mixed concretes, and the dashed lines represent the same in SW-mixed concretes. Figure 2a shows compressive strength development in binary blended concrete mixes with 30% fly ash, 50% slag, or 30% metakaolin produced with FW/SW mixing. In general, SW-mixed concretes of any binder combination had higher strength up to 28 days. The effect of SW mixing on increase in strength between 1 and 7 days was observed in CM30 compared to CC, CF30, and CS50 concretes due to the formation of hydrocalumite ($Ca_8Al_4(OH)_{24}(CO_3)Cl_2(H_2O)_{1.6}(H_2O)_8$), an intermediate solid solution between Friedel's salt and carboaluminate phases that can bind free chloride [37]. A marginal reduction in strength is observed at 91 days in binary blended SW concretes compared to their FW counterparts. This reduction in strength could be attributed to the possible

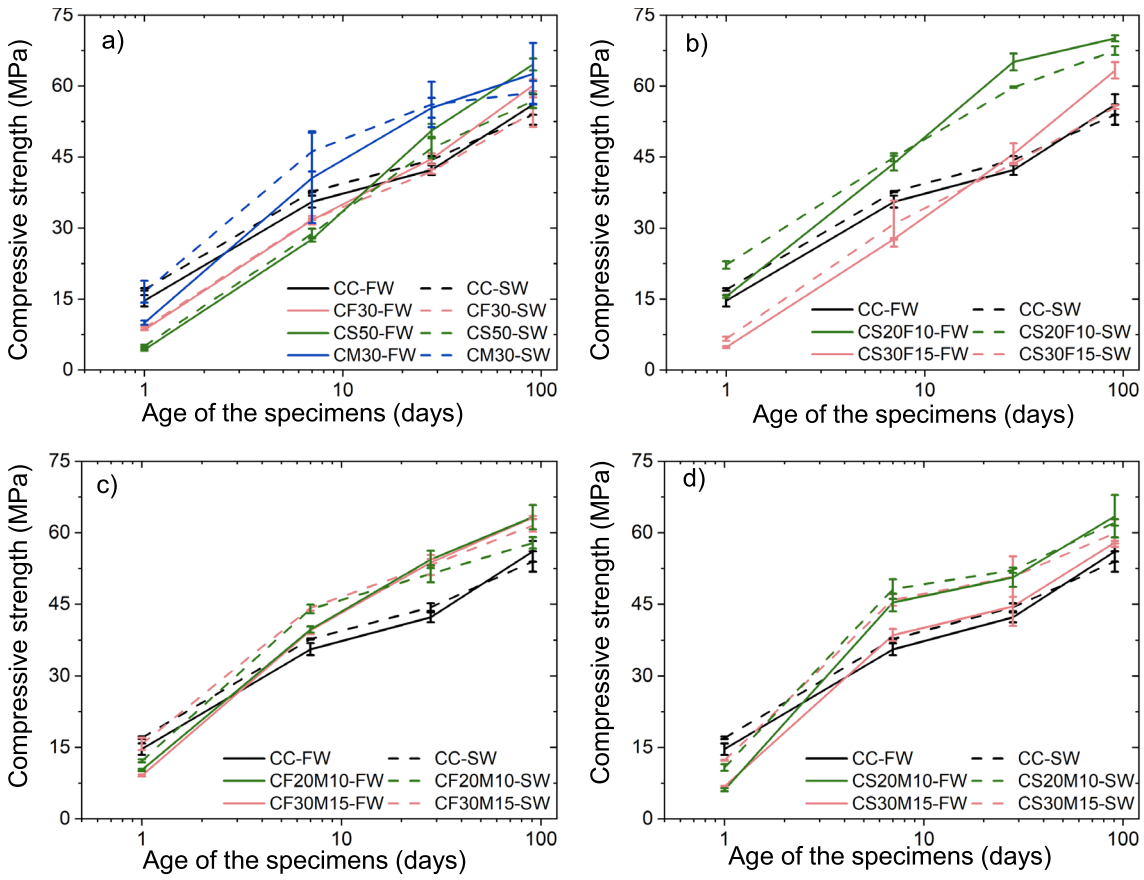

Fig. 2 Compressive strength development with time in seawater-mixed concretes made with CEM I and binary blends (**a**), CSxxFyy (**b**), CFxx-Myy (**c**), and CSxxMyy (**d**)

salt crystallisation effect due to higher ions in pore solution constituents of SW-mixed concrete [38] Notably, the long-term strength of these mixes, except CC-SW and CF30-SW, was higher than the control mix CC-FW.

Figure 2b shows the strength development in the ternary blend of CS20F10 and CS30F15 concretes mixed with both types of water. The dilution effect due to high-volume clinker substitution (45% by weight) led to a reduction in the rate of strength development in CS30F15-FW/SW, when compared to their CC concretes up to 28 days. However, the CS30F15-FW mix exhibited a more considerable strength gain at 91 days compared to other mixes' strength at 28 days due to continuous pozzolanic reaction of slag and fly ash expected to improve after 28 days [39]. The effect of SW mixing in strength gain is not observed well beyond seven days of hydration with the usage of fly ash and slag at higher replacement levels due to the hindering and clinker dilution effect affecting the later age pozzolanic activity [40].

Figure 2c and d show the results from ternary composition developed by blending metakaolin with CEM I and fly ash/slag. Adding metakaolin ensured a 50% increase in mean value of compressive strength with SW mixing (CM30-SW: 47 MPa) compared to the CC-FW (32 MPa) concrete at seven days and a 25% increase in strength compared to CM30-FW (38 MPa) concrete. The synergistic effect of metakaolin and ions in seawater ensured accelerated hydration and contributed to the improved pozzolanic reaction, which could be attributed to the increase in strength [41]. The combined effect of SW mixing and metakaolin substitution supported the pozzolanic reaction and produced C-S-H, C-A-H, C-A-S-H, and Friedel's salt that could densify the pore structure [42]. Furthermore, the addition of slag and fly ash in SW-mixed concretes with metakaolin ensured lesser reduction in strength at later age compared to the significant drop in strength observed in CM30 concrete at 91 days. Also, CS30M15-SW concrete showed a 5% improvement in strength later than its FW counterpart and CC-FW concretes, indicating the benefits of blending metakaolin with slag for adapting SW mixing.

Figure 3 summarises the relative improvement in compressive strength between the FW-mixed and SW-mixed concretes of the same composition concerning the age of the specimens. At 7 days, the increase in strength compared to FW mixing in ternary blended concrete lies between 10 and 25%. It is found that the beneficial effect of SW mixing is more pronounced in ternary blended concretes (CS30F15, CF30M15, and CS30M15) with 45% by weight of CEM I substitution in comparison to the other mixes. At 28 days, an improvement in compressive strength of up to 15% is found for the pair in CS30M15-SW vs CS30M15-FW, showing the compounding effect of these reactive SCMs in densifying the microstructure and developing strength through pozzolanic reaction [43]. At 91 days, it was observed that the replacement of FW with SW lead to a change in compressive strength between -15% and 5%, demonstrating the feasibility of producing SWCs having similar performance by optimising the binder composition.

4.2 Elastic modulus of concrete

Figure 4a and b show the elastic modulus (e-modulus) of all mixes after 1 and 91 days. Figure 4c indicates the increase in Young's modulus between 10 and 45% depending upon the binder type after one day of curing in SWCs compared to FWCs. This increase in e-modulus at an early age is attributed to the formation of denser microstructure at an early age [44], which results in stiffer concrete at younger age. Also, Fig. 4c shows that the effect of SW on the 1-day e-modulus is higher in concretes produced with metakaolin and slag blends that can have faster early-age hydration compared to concrete made with fly ash substitution. However, e-modulus values at 91 days concretes are similar, irrespective of the

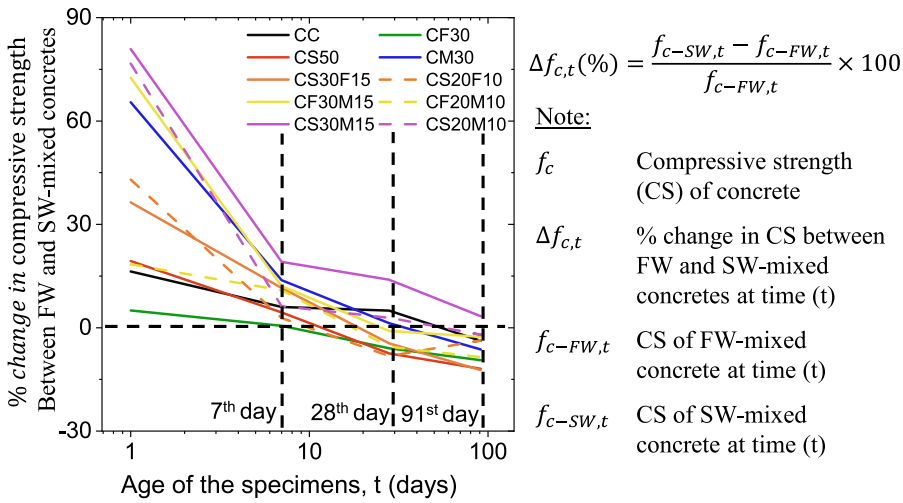

Fig. 3 Change (%) in compressive strength between FW and SW-mixed concretes up to 91 days

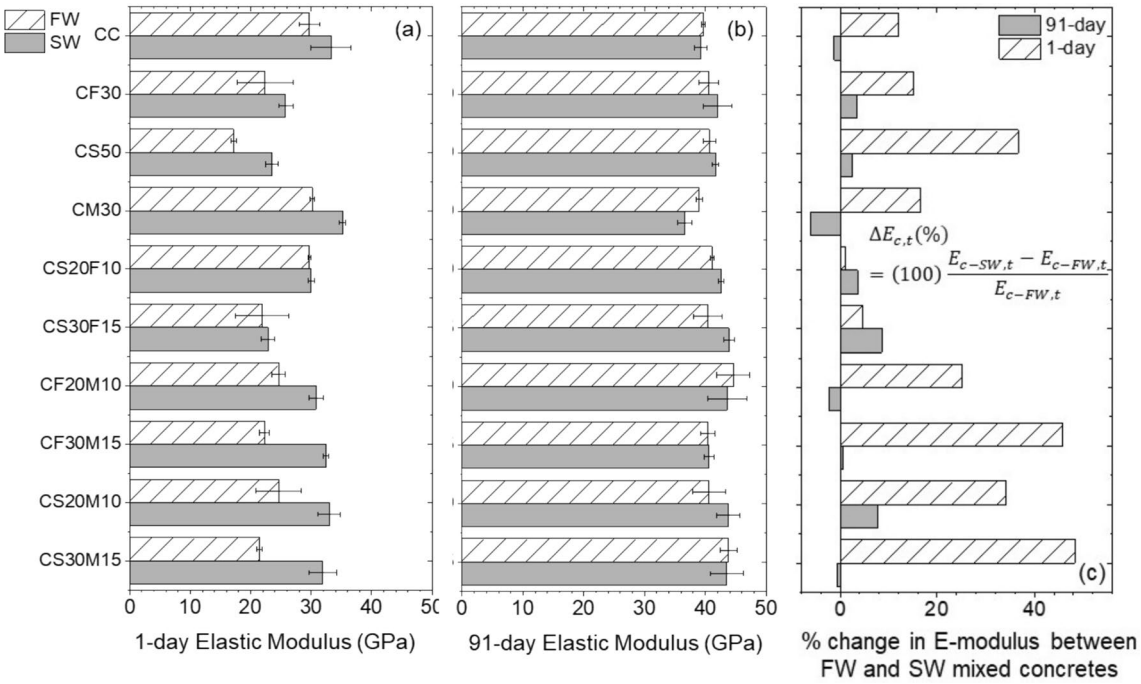

Fig. 4 Evolution of e-modulus in FW-mixed and SW-mixed specimens: 1 – day (**a**), 91st day (**b**), % change between FW and SW-mixed concrete cylinders (**c**)

type of binder and water used, as shown in Fig. 4b. At the same binder content (360 kg/m^3) and w/b (0.45), the SWCs have e-modulus ranging between 39 and 45 GPa, which is suitable for structural applications similar to FWCs exhibiting the e-modulus between 37 and 44 GPa. More research is required to evaluate the effect of SW mixing on long-term (> 1 year) mechanical and durability properties of concrete.

4.3 Electric resistivity measurements

An increase in the bulk and surface resistivity values was observed in the SWCs compared to the FWCs, as shown in Fig. 5a and b. The surface and bulk resistivity measurements were carried out on the same specimens at 1, 7, 28, and 91 days. The electrical resistivity of concrete can imply the likelihood of corrosion, as mentioned in Fig. 5a. Also, the surface resistivity measurements can be correlated with the chloride ion penetration resistance of the concrete conforming to the classification proposed in COST 509 report [45], as shown in Fig. 5b. The long-term durability of the concrete can be associated with its electrical resistivity, indirectly indicating the resistance to further ingress of chlorides, sulphates, and moisture [46].

The bulk and surface resistivity of the SWCs off all types of binder reach the classification of moderate likelihood of corrosion within seven days of curing. The 1-day resistivity values of all SW-mixed concrete except CM30 were lesser than those of the FW-mixed counterparts, which could be attributed to the presence of higher ionic concentration in the pore solution with seawater mixing [47]. A rapid increase in the resistivity values measured at seven days in SW-mixed concretes coincides with the formation of chloride binding phases like hydrocalumite and Friedel's salt between 48 and 100 h of hydration [48]. CM30-FW/SW concretes exhibit maximum resistivity, indicating the formation of denser microstructure with the possibility of achieving critical pore sizes as low as 8–16 nm [49].

The benefit of SW use in ternary concretes with metakaolin can be understood by the fact that surface resistivity values of CFxxMyy and CSxxMyy concretes at 28 days conform with the classification for lower likelihood of corrosion. Despite having higher cement replacement levels in CF30M15 and CS30M15 concretes, the use of SW resulted in a surface resistivity value of 50 kΩ.cm (which corresponds to the classification of lower likelihood of corrosion). Furthermore, in addition to the densification of microstructure with SCM substitution, the comparison between FWC and SWC of same blended combination shows the impact of accelerated hydration due to seawater mixing in improving the early-age resistivity values. Higher resistivity in SWCs is necessary to inhibit the further ingress of chlorides, sulphates, moisture, and carbonation, which would facilitate concrete deterioration. Except for CC concrete, the bulk and surface resistivity values of the other SW-mixed concretes are marginally higher at 91 days compared to their FW counterparts. The

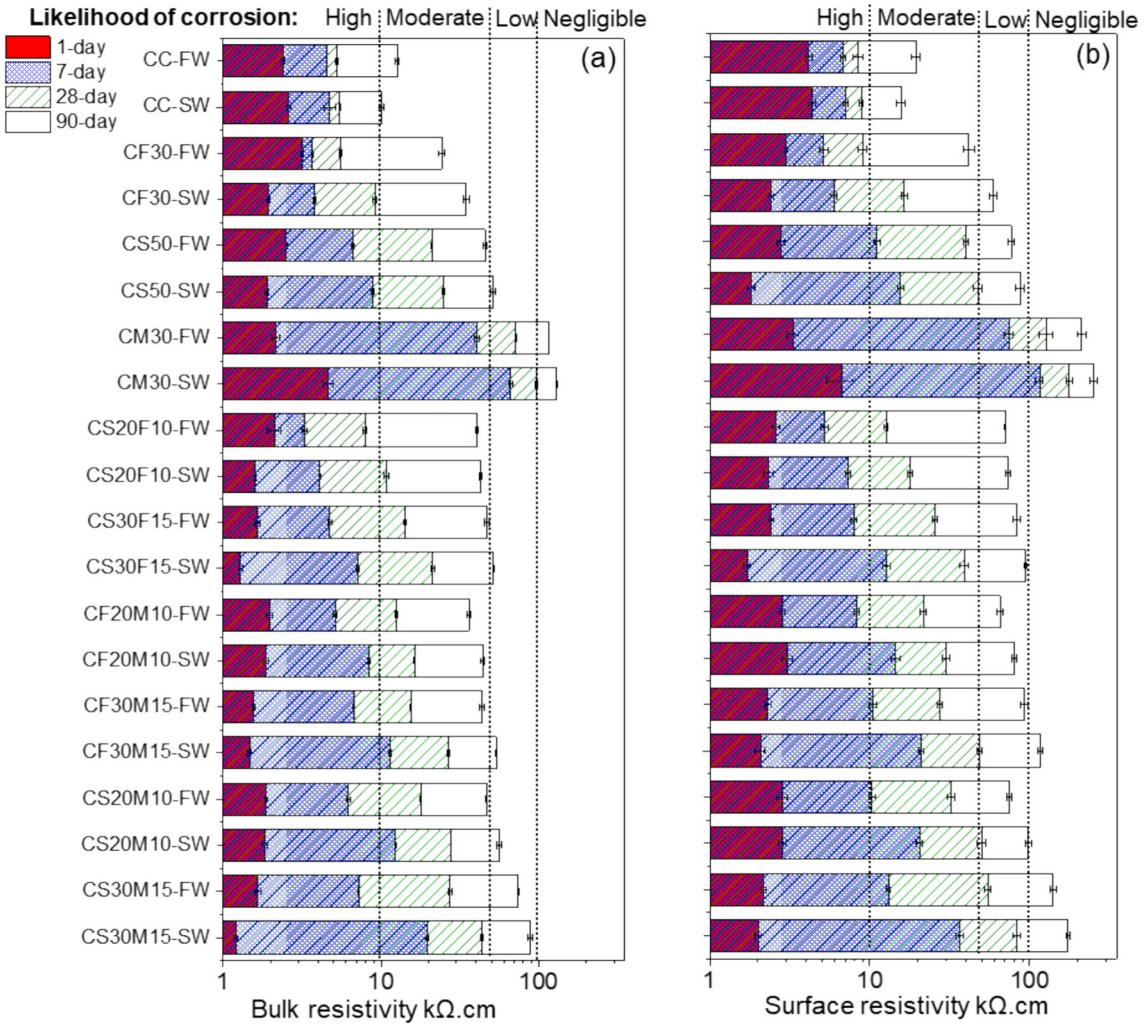

Fig. 5 Bulk resistivity (**a**) and surface resistivity (**b**) of FW-mixed and SW-mixed concretes

improvement in the resistivity in SWC indicates the lack of free chlorides or other ionic constituents of pore solution in the cementitious matrix [50].

Despite having a lower replacement level of metakaolin, the synergetic effect of slag and metakaolin contributes to accelerated hydration and pozzolanic action of CS30M15-FW/SW concrete, resulting in electrical resistivity values in the range of negligible likelihood of corrosion [43]. The faster gain in resistivity within 28 days in SW-mixed blended concretes with more than 30% cement replacement increases the potential of producing high-performance SWC for niche applications which is resistant to further chloride ingress from atmosphere. However, the stability of bound chlorides in low pH environments can alter the SWC resistivity in later ages due to carbonation or acid exposure. Desorption of chloride ions could be as high as 90% when the pH of concrete drops from 12 to 9 [51]. Hence, the impact of carbonation in SW-mixed concretes needs to be evaluated, particularly in the case of high-volume clinker replacement (> 30%) concretes.

4.4 Accelerated carbonation test

Figure 6 shows the results from accelerated carbonation tests in FW-mixed and SW-mixed concretes at 28 days. No discernible trends related to the use of SW were observed. There was a clear and expected trend for the concrete's carbonation depth to increase when the cement was replaced with SCMs. This observation is mainly attributed to the reduced formation of cement hydration products in the concrete because the SCMs are used as cement substitutes rather than additions [52]. This leads to a decrease of the amount of cement hydration products per volume of concrete and, for a given amount of CO_2 that penetrates concrete, the volume of carbonated concrete becomes larger [53]. Furthermore, some of the pozzolanic reactions of the SCMs (e.g. metakaolin

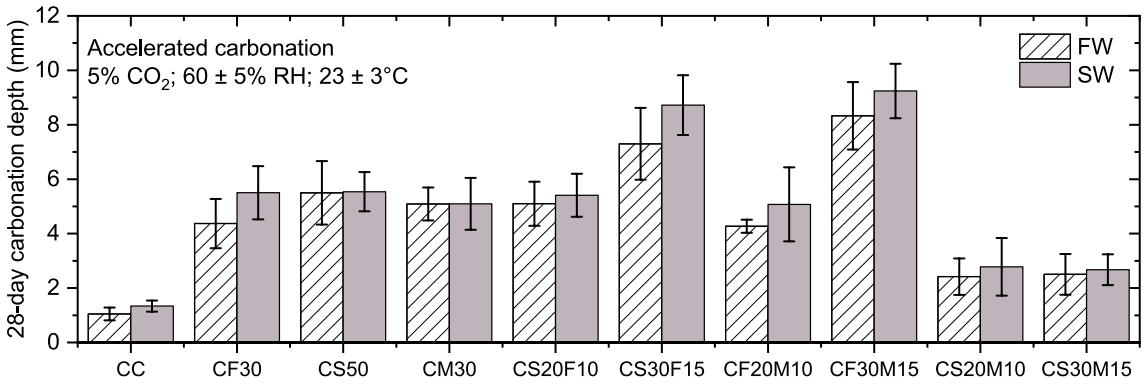

Fig. 6 Accelerated carbonation depth at 28 days

[54]) can consume portlandite, further contributing to this effect. Neville [55], based on research by Bier [56], confirms that the carbonation rate is higher in concretes with a lower $Ca(OH)_2$ content in the cement paste. This increase in carbonation rate in concretes with high-volume SCMs can lead to the risk of reversal of chemical and physical binding of chlorides from hydrated phases owing to their transformation into calcium carbonate under natural or accelerated carbonation process. A balance should be struck between the substitution of high-volume SCMs for chloride binding in concrete and its resistance to carbonation for optimising the binder composition suitable for producing SWCs.

There are considerable differences in the CO_2 penetration depth between the compositions using fly ash and blast furnace slag compared to the reference concrete (Fig. 6). These differences are significant, reaching up to four times higher carbonation depths for fly ash with 30% substitution and five times more for blast furnace slag. This trend is equally evident in mixes containing metakaolin, where the carbonation depth is up to five times that of the reference concrete. Concerning the two groups of ternary mixes analysed, the first group combines cement, blast furnace slag, and fly ash, with 20 to 30% and 10 to 15% substitution, respectively. In the second group, cement is partially replaced by fly ash/blast furnace slag and metakaolin, in proportions of 20 to 30% and 10 to 15%.

An increase in carbonation penetration was observed in both cases compared to the reference concrete mix for the same reasons mentioned above—see Rivera et al. [57] in their research with ternary mixes of cement, fly ash, and blast furnace slag. In the ternary mix with cement, blast furnace slag, and metakaolin, the increase in carbonation depth is smaller than that observed for the concrete made with the ternary blend with blast furnace slag and fly ash. Bai et al. [58] found contradictory results in their research with ternary mixes of cement, pulverised ash, and metakaolin, attributing the reduction in carbonation depth to the low calcium hydroxide content in mixed concretes with binders. The lesser carbonation depth in CS20M10 and CS30M15 concretes indicates the higher CaO buffer in the solution with slag. The synergy between the higher resistivity and CaO buffer in these mixes ensured a lower carbonation depth after 28 days in an accelerated carbonation environment, thus reducing the risk of reversal of chloride binding.

5 Life cycle assessment

A life cycle assessment (LCA) was conducted to quantify the environmental benefits of replacing freshwater with seawater in concrete production. The functional unit chosen was 1 m^3 of concrete. The LCA is carried out for the Chennai region of India. The environmental impacts were calculated in agreement with EN 15804 + A2 [59], using the method "V1.01 / EF 3.1 normalisation and weighting set" of the software SimaPro 9.6.0.1. Two environmental impact categories were studied: the water depletion potential (WDP) – AWARE (Available WAter REmaining), and Global warming potential (GWP) – Environmental Footprint 3.1. AWARE is a midpoint indicator that accounts for water consumption in relation to the available water in a region after the demand for humans and aquatic ecosystems is accounted for. For a given water use, the less water is available in a region, the higher its WDP is, according to AWARE.

The LCA is made from cradle-to-gate and the information modules [59] included are A1 (raw material production), A2 (transport of raw materials to production site), and A3. Life cycle stage A3 (production of the concrete mixes) is omitted for simplification since this information module i) represents a negligible portion of the life cycle environmental impacts of concrete [60] and ii) is the same for all mixes studied in the paper, since production (mixing and other ancillary activities) is unaffected by the type of binder or water. For each raw material, the inventory is sourced from secondary data from i) Environmental Product Declarations (EPDs), ii) the Ecoinvent database

[61], and iii) peer-reviewed publications. Table 3 shows the sources of data. In the case of the Ecoinvent database, the processes were adapted to the Chennai (Tamil Nadu) region using the following processes to replace the generic ones:

- Electricity: Electricity, medium voltage {IN-Southern grid} | market for electricity, medium voltage | Cut-off, U.
- Water: Water, unspecified natural origin, IN-TN.

Chennai was selected for the life cycle assessment due to its potential of becoming a megacity in the near future considering its active infrastructural development and also because it is facing a threat of severe water stress. Furthermore, the availability of supplementary cementitious materials like fly ash, slag, and metakaolin and their continuous supply is expected to last much longer in this region compared to cities in Europe which focus more on shutting down thermal power and steel production plants. The information module 2 (transport of raw materials to Chennai) was determined based on the transport distances presented in Table 4, and the environmental modelling assumed transport was carried out by a 32-tonne truck.

The ready-mixed plant is located near a saltwater source and infrastructural needs to adapt the ready-mixed plant for saltwater were modelled, but its impacts are assumed to be negligible when compared to the impacts of ready-mixed concrete production, as commonly done in LCA for concrete production that require small infrastructural adaptations. These transport distances and raw materials are associated with the GWP and WDP, as stated in Table 5 for information modules A1 and A2.

The GWP is presented in Fig. 7. The following is concluded:

Table 4 Transport distances of the raw materials

Material	Information about the source of raw materials from Chennai	
	Location	Distance (km)
CEM I	Nandyal/Arakkonam	400
Fly ash	Ennore	50
Slag	Vijayanagar	550
Metakaolin	Trivandrum	900
Superplasticiser	Mumbai	1100
Coarse aggregate	Kanchipuram	100
River sand	Villupuram/Palar basin	200

- As expected, the replacement of cement with SCMs results in significant decreases in GWP. It is a direct consequence of the high GWP associated with cement production (see the A1 impacts presented in Table 4) due to the significant impacts associated with limestone calcination for clinker production.
- From the previous point, the results show that cement content and GWP are strongly correlated (correlation coefficient of 0.88).
- Regarding replacing freshwater with seawater, negligible differences in GWP are reported. As understood from the mix designs presented in Table 2, the only change to the mix design due to the replacement of freshwater by seawater is the increase of SP content (by an amount of up to 13%). These changes to the mix design are irrelevant when compared to the total GWP of the mixes.

Very relevant differences are observed when the WDP is analysed, as indicated in Fig. 8:

- The replacement of cement with SCM influences GWP relevantly due to the differences in the values of WDP of

Table 3 Sources and references for life cycle impacts

Raw material	Source	References
Cement CEM I 42.5 R	EPD—CEMBUREAU	[62]
Fly ash	EPD—Emineral A/s	[63]
Slag	EPD—Kuwait cement company	[64]
Metakaolin	Ecoinvent—Calcined clay {RoW}| calcined clay production	Cut-off, U	[61]
PCE Superplasticiser	Publication—Hájek et al	[65]
Coarse aggregates	Ecoinvent—Gravel, crushed {IN}| gravel production, crushed	Cut-off, U	[61]
Sand 0/2	Ecoinvent—Sand 0/2 mm, wet and dry quarry, production mix, at the plant, undried RER S	[61]
Transport	Ecoinvent—Transport, freight, lorry > 32 metric tonne, EURO4 {RoW}| market for transport, freight, lorry > 32 metric tonne, EURO4	Cut-off, U	[61]
Freshwater	Ecoinvent—Water, unspecified natural origin, IN-TN	[61]
Seawater	Ecoinvent—Process based on “market for tap water IN” and “tap water production, underground water without treatment IN” with the input from nature changed to “Water, salt, ocean”	[61]

Table 5 GWP and WDP by a tonne of each raw material

Raw material	A1		A2		A1 + A2	
	GWP ($kgCO_2eq.$)	WDP (m^3)	GWP ($kgCO_2eq.$)	WDP (m^3)	GWP ($kgCO_2eq.$)	WDP (m^3)
Cement CEM I 42,5 R	803	14.1	31.7	0.4	834.7	14.5
Fly ash	0.001	0.04	4.0	0.05	4.0	0.1
Slag	281.0	24.7	43.6	0.5	324.6	25.2
Metakaolin	273.3	5.85	71.3	0.9	344.6	6.7
PCE Superplasticiser	2730	7.4	87.1	1.1	2817.1	8.5
Coarse aggregates	6.8	0.9	7.9	1.0	14.7	1.9
Sand 0/2	5.0	0.4	15.8	0.2	20.8	0.3
Freshwater	1.1	28.96	–	–	1.1	28.96
Sea water	0.5	0.07	–	–	0.5	0.07

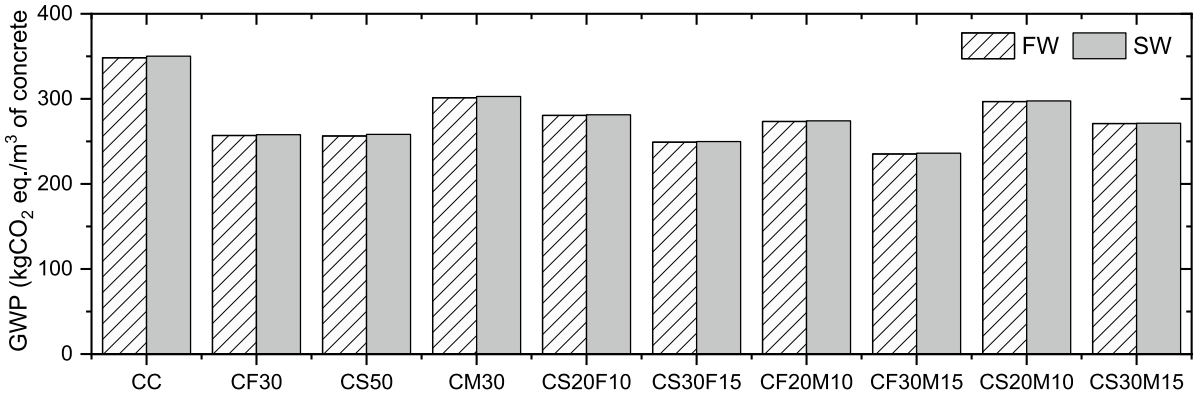

Fig. 7 Global warming potential (GWP) of fresh and seawater-mixed concretes

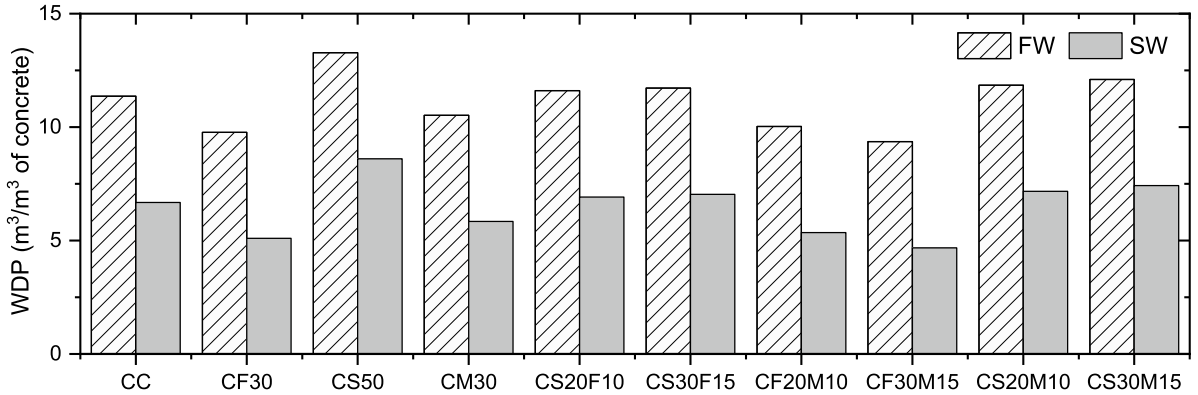

Fig. 8 Water depletion potential of fresh and seawater-mixed concretes

the SCMs (Table 4): slag has a higher WDP than cement, while that of metakaolin is roughly half the WDP of cement. The WDP of fly ash is virtually nil.

- The replacement of FW by SW results in a very meaningful reduction of WDP in all cases, ranging between 35 and 50%. It occurs because freshwater is replaced with seawater, which results in a WDP of roughly 4.5 m^3 for all compositions. The more considerable relative differences are reported for the compositions made with fly ash (CF30 and CF30M15) since these are the ones with the smaller GWP.

- Similar findings were reported in another publication developed within [30] this project's scope [29], in which the relative decrease of WDP of lightweight aggregate concrete due to the replacement of freshwater with seawater was about 30%.

For other regions, different findings may be observed, not only due to differences in transport distances and raw materials but also because of the local character of the WDP – AWARE indicator.

6 Conclusions

The experimental results of macro-scale properties and life cycle assessment of SW-mixed concrete were presented, and the following inference can be drawn from this study.

- Up to 7 days, the compressive strength of concrete mixes made with SW is significantly higher than that of concrete made with FW. The CS30M15-SW concrete had the highest relative increase of 7-day compressive strength compared to its FW counterpart.
- The synergetic effect of metakaolin and slag densified the microstructure and enhanced the chloride binding, resulting in higher bulk and surface resistivity in CS30M15 concrete compared to other concretes considered in this study. However, the associated risks of higher hydration heat, shrinkage, microcracking, and the interaction of aluminate hydrated phases with high temperature or moisture due to the presence of higher Al_2O_3 content in binder composition should be investigated further.
- The improved resistivity and significantly higher CaO buffer in CS30M15 and CS20M10 concrete resulted in a lower carbonation depth and, hence, reduced risk of reversal of chloride binding.
- The replacement of FW by SW has negligible effects in the GWP but contributes very meaningfully towards reducing the WDP of concrete. Under the conditions of this case study (Chennai, India), the relative decrease of WDP was always in the region of 35% to 50%. Fly ash has a lesser energy requirement than other materials; thus, the CF30 and CF30M15 mixes show much less WDP.

Hence, this study recommends that ternary combinations with slag and fly ash with metakaolin are suitable for producing strong, durable, and sustainable SWC. Future research should be directed towards the long-term durability performance of SWCs in accelerated and natural exposure conditions including chloride-rich, sulphate-rich, and acidic environments. Additional research on chemical and physical chloride binding behaviour of hydrated cement phases shall be conducted to estimate the risk of available free chlorides content at the reinforcement–cementitious interface exceeding the critical chloride threshold of types of steel (coated, galvanised, or corrosion resistant) to be used in structural applications of SW-mixed concretes.

Acknowledgements This research is part of project No. 2021/43/P/ST8/00945, co-funded by the National Science Centre and the European Union Framework Program for Research and Innovation Horizon 2020 under the Marie Sklodowska-Curie grant agreement No. 945339. The authors also acknowledge the support of the Portuguese Foundation for Science and Technology through the funding UIDB/04625/2020 of the CERIS research unit (https://doi.org/10.54499/UIDB/04625/2020) and the funding of c5Lab by the Interface Mission [01/C05-i02/2022.P264].

Authors' contributions Conceptualization, Investigation, Writing Original draft and preparation, Formal analysis, Funding acquisition: SR. Formal analysis, writing review and editing, Funding acquisition: JNP. Conceptualization, writing review and editing, and Supervision: PS. Formal analysis, Investigation, and Methodology (Life cycle assessment): FC. Investigation, Methodology: MT, JV.

Data availability Data will be made available on request.

Declarations

Conflict of interest The authors have no competing interests to declare that are relevant to the content of this article.

Open Access This article is licensed under a Creative Commons Attribution 4.0 International License, which permits use, sharing, adaptation, distribution and reproduction in any medium or format, as long as you give appropriate credit to the original author(s) and the source, provide a link to the Creative Commons licence, and indicate if changes were made. The images or other third party material in this article are included in the article's Creative Commons licence, unless indicated otherwise in a credit line to the material. If material is not included in the article's Creative Commons licence and your intended use is not permitted by statutory regulation or exceeds the permitted use, you will need to obtain permission directly from the copyright holder. To view a copy of this licence, visit http://creativecommons.org/licenses/by/4.0/.

References

1. World Water Assessment Programme (United Nations), UN-Water, Unesco, Water for prosperity and peace, n.d.
2. Kuzma S, Saccoccia L, Chertock M. 25 Countries, Housing One-quarter of the Population, Face Extremely High Water Stress Get water-related insights from WRI sent straight to your inbox, 2023.
3. Wada Y, Flörke M, Hanasaki N, Eisner S, Wada Y, Flörke M, Hanasaki N, Eisner S, Fischer G, Tramberend S, Satoh Y, Van Vliet MTH, Yillia P, Ringler C, Burek P, Wiberg D. Modeling global water use for the 21st century: Water Futures and Solutions (WFaS) initiative and its approaches Modeling global water use for the 21st century: the Water Futures and Solutions (WFaS) initiative and its approaches. Geosci Model Dev. 2016;9:175–222. https://doi.org/10.5194/gmdd-8-6417-2015.
4. Boretti A, Rosa L. Reassessing the projections of the World Water Development Report. NPJ Clean Water. 2019. https://doi.org/10.1038/s41545-019-0039-9.

5. Miller SA, Horvath A, Monteiro PJM. Impacts of booming concrete production on water resources worldwide. Nat Sustain. 2018;1:69–76. https://doi.org/10.1038/s41893-017-0009-5.
6. EN 1008, Mixing water for concrete. Specification for sampling, testing and assessing the suitability of water, including water recovered from processes in the concrete industry, as mixing water for concrete., 2002.
7. Rathnarajan S, Sikora P. Seawater-mixed concretes containing natural and sea sand aggregates—a review. Results Eng. 2023;20: 101457. https://doi.org/10.1016/j.rineng.2023.101457.
8. Jackson MD, Moon J, Gotti E, Taylor R, Chae SR, Kunz M, Emwas AH, Meral C, Guttmann P, Levitz P, Wenk HR, Monteiro PJM. Material and elastic properties of Al-tobermorite in ancient roman seawater concrete. J Am Ceram Soc. 2013;96:2598–606. https://doi.org/10.1111/jace.12407.
9. Ashraf W, Borno IB, Khan RI, Siddique S, Haque MI, Tahsin A. Mimicking the cementation mechanism of ancient Roman seawater concrete using calcined clays. Appl Clay Sci. 2022. https://doi.org/10.1016/j.clay.2022.106696.
10. Thomas MDA, Hooton RD, Scott A, Zibara H. The effect of supplementary cementitious materials on chloride binding in hardened cement paste. Cem Concr Res. 2012;42:1–7. https://doi.org/10.1016/j.cemconres.2011.01.001.
11. Khatibmasjedi M, Ramanathan S, Suraneni P, Nanni A. Compressive strength development of seawater-mixed concrete subject to different curing regimes. ACI Mater J. 2020;117:3–12. https://doi.org/10.14359/51725973.
12. Xie Q, Xiao J, Zhang K, Zong Z. Compressive behavior and microstructure of concrete mixed with natural seawater and sea sand, Frontiers of Structural and Civil. Engineering. 2021;15:1347–57. https://doi.org/10.1007/s11709-021-0780-2.
13. Wang J, Liu E, Li L. Multiscale investigations on hydration mechanisms in seawater OPC paste. Constr Build Mater. 2018;191:891–903. https://doi.org/10.1016/j.conbuildmat.2018.10.010.
14. Younis A, Ebead U, Suraneni P, Nanni A. Fresh and hardened properties of seawater-mixed concrete. Constr Build Mater. 2018;190:276–86. https://doi.org/10.1016/j.conbuildmat.2018.09.126.
15. Wang J, Xie J, Wang Y, Liu Y, Ding Y. Rheological properties, compressive strength, hydration products and microstructure of seawater-mixed cement pastes. Cem Concr Compos. 2020. https://doi.org/10.1016/j.cemconcomp.2020.103770.
16. Alomayri T, Amir MT, Ali B, Raza SS, Hamad M. Mechanical, tidal erosion, and drying shrinkage behaviour of high performance seawater concrete incorporating the high volume of GGBS and polypropylene fibre. J Build Eng. 2023;76: 107377. https://doi.org/10.1016/j.jobe.2023.107377.
17. Sikora P, Lootens D, Liard M, Stephan D. The effects of seawater and nanosilica on the performance of blended cements and composites. Appl Nanosci (Switzerland). 2020;10:5009–26. https://doi.org/10.1007/s13204-020-01328-8.
18. Liu J, An R, Jiang Z, Jin H, Zhu J, Liu W, Huang Z, Xing F, Liu J, Fan X, Sui T. Effects of w/b ratio, fly ash, limestone calcined clay, seawater and sea-sand on workability, mechanical properties, drying shrinkage behavior and micro-structural characteristics of concrete. Constr Build Mater. 2022. https://doi.org/10.1016/j.conbuildmat.2022.126333.
19. Cai HM, Qing WU, Shen L. Research on frost resistance of seawater sea-stone concrete. In: IOP Conf Ser Earth Environ Sci, Institute of Physics Publishing, 2019. https://doi.org/10.1088/1755-1315/267/5/052001.
20. Zhang Y, Xu X, Zhao Q, Chang J, Ding S, Liu X, Poon CS. Long-term investigation of alkali-silica reaction behaviors in seawater sea-sand concrete. Cem Concr Compos. 2024. https://doi.org/10.1016/j.cemconcomp.2024.105611.
21. De Weerdt K. Chloride binding in concrete: recent investigations and recognised knowledge gaps: RILEM Robert L'Hermite Medal Paper 2021, Materials and Structures/Materiaux et Constructions 54 (2021). https://doi.org/10.1617/s11527-021-01793-9.
22. Ji Y, Zhang X, Pel L, Sun Z. NMR investigations on Cl− and Na+ ion binding during the early hydration process of C3S, C3A and cement paste: a combined modelling and experimental study. Compos B Eng. 2024. https://doi.org/10.1016/j.compositesb.2024.111624.
23. Zhao Y, Hu X, Yuan Q, Wu Z, Shi C. Effects of water to binder ratio on the chloride binding behaviour of artificial seawater cement paste blended with metakaolin and silica fume. Constr Build Mater. 2022. https://doi.org/10.1016/j.conbuildmat.2022.129110.
24. Guo B, Qiao G, Han P, Li Z, Fu Q. Effect of natural carbonation on chloride binding behaviours in OPC paste investigated by a thermodynamic model. J Build Eng. 2022. https://doi.org/10.1016/j.jobe.2022.104021.
25. Dasar A, Patah D, Hamada H, Sagawa Y, Yamamoto D. Applicability of seawater as a mixing and curing agent in 4-year-old concrete. Constr Build Mater. 2020. https://doi.org/10.1016/j.conbuildmat.2020.119692.
26. Jiang Z, Li S, Fu C, Dong Z, Zhang X, Jin N, Xia T. Macrocell corrosion of steel in concrete under carbonation, internal chloride admixing and accelerated chloride penetration conditions. Materials. 2021. https://doi.org/10.3390/ma14247691.
27. Pan C, Li X, Mao J. The effect of a corrosion inhibitor on the rehabilitation of reinforced concrete containing sea sand and seawater. Materials. 2020. https://doi.org/10.3390/ma13061480.
28. Sikora P, Afsar L, Rathnarajan S, Nikravan M, Chung SY. Seawater—mixed lightweight aggregate concretes with dune sand, waste glass and nanosilica: experimental and life cycle analysis. Int J Concr Struct Mater. 2023. https://doi.org/10.1186/s40069-023-00613-4.
29. Rathnarajan S, Cendrowski K, Sibera D, Sikora P. Comprehensive evaluation of early-age hydration and compressive strength development in seawater-mixed binary and ternary cementitious systems. Arch Civ Mech Eng. 2024. https://doi.org/10.1007/s43452-024-00932-7.
30. EN 197 - Part I, Cement. Part 1, Composition, specifications and conformity criteria for common cements. BSI, 2000.
31. ASTM-D1141-98, Standard Practice for Preparation of Substitute Ocean Water (1998).
32. British Standards Institution, EN 12350-–2 - Testing fresh concrete: Slump test, 2009.
33. British Standards Institution., Testing hardened concrete. Part 3, Compressive strength of test specimens., BSI, 2002.
34. British Standards Institution. Testing hardened concrete. Part 13, Determination of secant modulus of elasticity in compression, 2013.
35. Standard Method of Test for Surface Resistivity Indication of Concrete's Ability to Resist Chloride Ion Penetration American Association of State Highway and Transportation Officials, 2015. www.salmanco.comwww.salmanco.com.
36. LNEC E 391 specification: concrete - determination of resistance to carbonation, LNEC Portugal, 1993.
37. Li Q, Geng H, Shui Z, Huang Y. Effect of metakaolin addition and seawater mixing on the properties and hydration of concrete. Appl Clay Sci. 2015;115:51–60. https://doi.org/10.1016/j.clay.2015.06.043.
38. Wegian FM. Effect of seawater for mixing and curing on structural concrete. IES J Part A. 2010;3:235–43. https://doi.org/10.1080/19373260.2010.521048.
39. Dehuai W, Zhaoyuan C. On predicting compressive strengths of mortars with ternary blends of cement, GGBFS and fly ash. Cem

Concr Res. 1997;27(4):487–93. https://doi.org/10.1016/S0008-8846(97)00039-2.
40. Zhao Y, Hu X, Shi C, Zhang Z, Zhu D. A review on seawater sea-sand concrete: mixture proportion, hydration, microstructure and properties. Constr Build Mater. 2021. https://doi.org/10.1016/j.conbuildmat.2021.123602.
41. Shi Z, Shui Z, Li Q, Geng H. Combined effect of metakaolin and sea water on performance and microstructures of concrete. Constr Build Mater. 2015;74:57–64. https://doi.org/10.1016/j.conbuildmat.2014.10.023.
42. Li Q, Geng H, Huang Y, Shui Z. Chloride resistance of concrete with metakaolin addition and seawater mixing: a comparative study. Constr Build Mater. 2015;101:184–92. https://doi.org/10.1016/j.conbuildmat.2015.10.076.
43. Li Z, Ding Z. Property improvement of Portland cement by incorporating with metakaolin and slag. Cem Concr Res. 2003;33:579–84. https://doi.org/10.1016/S0008-8846(02)01025-6.
44. Pan D, Yaseen SA, Chen K, Niu D, Ying Leung CK, Li Z. Study of the influence of seawater and sea sand on the mechanical and microstructural properties of concrete. J Build Eng. 2021;42:103006. https://doi.org/10.1016/j.jobe.2021.103006.
45. Cox RN, Cigna R, Vennesland O, Valente T. COST 509 corrosion and protection of metals in contact with concrete F, Brussels, 1997.
46. Dhandapani Y, Sakthivel T, Santhanam M, Gettu R, Pillai RG. Mechanical properties and durability performance of concretes with Limestone Calcined Clay Cement (LC3). Cem Concr Res. 2018;107:136–51. https://doi.org/10.1016/j.cemconres.2018.02.005.
47. Montanari L, Suraneni P, Tsui-Chang M, Khatibmasjedi M, Ebead U, Weiss J, Nanni A. Hydration, pore solution, and porosity of cementitious pastes made with seawater. J Mater Civ Eng. 2019. https://doi.org/10.1061/(asce)mt.1943-5533.0002818.
48. Ming X, Li Y, Liu Q, Wang M, Cai Y, Chen B, Li Z. Chloride binding behaviors and early age hydration of tricalcium aluminate in chloride-containing solutions. Cem Concr Compos. 2023. https://doi.org/10.1016/j.cemconcomp.2023.104928.
49. Homayoonmehr R, Ramezanianpour AA, Mirdarsoltany M. Influence of metakaolin on fresh properties, mechanical properties and corrosion resistance of concrete and its sustainability issues: a review. J Build Eng. 2021. https://doi.org/10.1016/j.jobe.2021.103011.
50. Lübeck A, Gastaldini ALG, Barin DS, Siqueira HC. Compressive strength and electrical properties of concrete with white Portland cement and blast-furnace slag. Cem Concr Compos. 2012;34:392–9. https://doi.org/10.1016/j.cemconcomp.2011.11.017.
51. Long WJ, Zhang X, Feng GL, Xie J, Xing F, Dong B, Zhang J, Khayat KH. Investigation on chloride binding capacity and stability of Friedel's salt in graphene oxide reinforced cement paste. Cem Concr Compos. 2022. https://doi.org/10.1016/j.cemconcomp.2022.104603.
52. de Medeiros MHF, Raisdorfer JW, Hoppe Filho J, Medeiros-Junior RA. Partial replacement and addition of fly ash in Portland cement: influences on carbonation and alkaline reserve. J Build Pathol Rehabil. 2017. https://doi.org/10.1007/s41024-017-0023-z.
53. Chindaprasirt P, Rukzon S. Pore structure changes of blended cement pastes containing fly ash, rice husk ash, and palm oil fuel ash caused by carbonation. J Mater Civ Eng. 2009;21:666–71. https://doi.org/10.1061/(ASCE)0899-1561(2009)21:11(666).
54. Gruyaert E, Van Den Heede P, De Belie N. Carbonation of slag concrete: effect of the cement replacement level and curing on the carbonation coefficient—effect of carbonation on the pore structure. Cem Concr Compos. 2013;35:39–48. https://doi.org/10.1016/j.cemconcomp.2012.08.024.
55. Neville AM. Properties of concrete. 4th edition, Prentice Hall; London; 1995.
56. Bier TA. Influence of type of cement and curing on carbonation progress and pore structure of hydrated cement pastes. In: MRS Online Proceedings Library (OPL), 1986; pp. 123–30.
57. Rivera RA, Sanjuán MÁ, Martín DA. Granulated blast-furnace slag and coal fly ash ternary portland cements optimization. Sustainability (Switzerland). 2020;12:1–15. https://doi.org/10.3390/su12145783.
58. Bai J, Wild S, Sabir BB. Sorptivity and strength of air-cured and water-cured PC-PFA-MK concrete and the influence of binder composition on carbonation depth, Cem Concr Res. 2002;32(11):1813–21. https://doi.org/10.1016/S0008-8846(02)00872-4.
59. EN-15804: 2012 + A2:2019 - Sustainability of construction works - Environmental product declarations - Core rules for the product category of construction products, 2019.
60. Braga AM, Silvestre JD, de Brito J. Compared environmental and economic impact from cradle to gate of concrete with natural and recycled coarse aggregates. J Clean Prod. 2017;162:529–43. https://doi.org/10.1016/j.jclepro.2017.06.057.
61. EcoEcoinvent LCA database v3.8, Swiss Centre for Life Cycle Inventories (2023).
62. Environmental Product Declaration according to EN 15804 and ISO 14025: Portland Cement (CEM I) produced in Europe, Brussels, 2020.
63. Environmental Product Declaration in accordance with ISO 14025 and EN 15804: Fly ash, Copen hagen, 2020. http://echa.europa.eu/candidate-list-table.
64. Environmental Product Declaration: In accordance with ISO 14025 AND EN15804: Ground Granulated Blast Furnace Slag, 2022. www.environdec.com.
65. Hájek P, Fiala C, Kynčlová M. Life cycle assessments of concrete structures—a step towards environmental savings. Struct Concr. 2011;12:13–22. https://doi.org/10.1002/suco.201000026.

Publisher's Note Springer Nature remains neutral with regard to jurisdictional claims in published maps and institutional affiliations.